Electrochemical Investigation of Traps in a Nanostructured TiO_2 Film

Heli Wang, Jianjun He, Gerrit Boschloo, Henrik Lindström, Anders Hagfeldt, and Sten-Eric Lindquist*

Department of Physical Chemistry, University of Uppsala, S-75121 Uppsala, Sweden

Received: October 3, 2000; In Final Form: January 6, 2001

Electron traps at the nanostructured TiO_2 (anatase)/aqueous electrolyte interface have been studied by means of electrochemical methods. The transient current decays at different potentials positive of the flat band potential clearly illustrate the trap-filling process. The more negative the potential, the shorter the trap-filling period. It is found that most traps locate positive of −0.9 V vs Ag/AgCl at pH 13, or positive of −0.3 V vs Ag/AgCl at pH 4.7. It is proposed that the trap distribution as a function of potential is directly proportional to dQ/dU, i.e., to the current density in a linear sweep voltammetry experiment. The trap densities in aqueous electrolytes are estimated to be 4×10^{11} cm^{-2} (microscopic area) at pH 4.7 and 5×10^{13} cm^{-2} (microscopic area) at pH 13. The pH dependency of the trap density indicates that traps investigated are surface-related.

Introduction

Nanostructured (or nanoporous−nanocrystalline) semiconductor electrodes composed of small, interconnected semiconductor particles (typically less than 100 nm in size) have attracted considerable interest.[1−12] The nanostructured film can have an effective surface area that can be enhanced 1000-fold compared to the projected geometric area.[6] This provides a base for different possible applications, since the reaction rate per unit projected area at a nanostructured electrode can be increased. On the other hand, the enhanced surface area and the interconnected particles give rise to a large number of electron traps at the nanostructured semiconductor/electrolyte interface (NSEI) and the grain boundaries, which may affect the interfacial kinetics.

Traps, including surface states, are electronic energy levels located in the band gap. In a dye-sensitized solar cell upon illumination, trapping of electrons in the TiO_2 particle leads to a lower position of the quasi-Fermi level of electrons and thus the output photovoltage is reduced. Electron trapping can also be considered as a "doping process" and the conductivity of the electrode can therefore be improved under trap-filled conditions.[13] Photoconductivity is explained in this way. Traps are extensively involved in the charge-transport process in nanostructured semiconductor films. Moreover, it has been proposed that the charge transport in such films is dominated by the mechanism of trapping/detrapping.[3,8,13−17]

Trapped electrons in nanostructured TiO_2 have been extensively studied.[3,7,8,13−16,18−25] The chemical nature of a localized energy level just below the conduction band (CB) edge is well established as the Ti^{3+}(3d) state.[20,26] The effects of traps in nanostructured semiconductor electrodes are apparent from measurements of photocurrent,[3,7,17,27,28] photovoltage,[8,27] charge recombination kinetics,[23,27] transient photoconduction,[13] spectroelectrochemical response,[2,14,21,22,26] and cyclic voltammetry.[27,29]

Since the traps are energetically located below the CB edge of the semiconductor, they can be filled either by band gap illumination with enough intensity or by means of an external bias. In the latter case, the Fermi level of the semiconductor is kept constant with a potentiostat; thus all the traps with energetic levels below this controlled Fermi level can be filled if the filling time is satisfied. Previous studies on photocurrent transients and absorption transients with particulate electrodes show typical times in the range of milliseconds to seconds.[3,7,22−25] The time resolution of a potentiostat can normally satisfy measurement on such a time scale and can register the transient signal. In this paper, it is shown that the observation of the trap-filling process at potentials positive of the flat band potential (U_{FB}) by means of transient current decay can be performed, giving an insight into the trap distribution in a nanostructured TiO_2 film electrode.

Experimental Section

1. Preparations of Electrodes and Electrolytes. Colloidal TiO_2 solution (Solaronix D) was purchased from Solaronix S.A. According to the supplier's specification the solid particle size is around 13 nm. Nanostructured TiO_2 films were prepared on a conducting glass substrate (F-doped SnO_2; sheet resistance 10−15 Ω/□), using Scotch tape as a spacer, by deposition of the colloidal TiO_2 solution and raking off the excess suspension with a glass rod. The films were dried and then heated at 450 °C for 1 h in air. The thickness of the films was controlled in the deposition stage by spacing Scotch tapes, and was checked after the sintering by using a step profiler (Sloan Dektak 3). We used 5.0 μm thick TiO_2 films in this report. The films were cut into pieces, and electrodes with a projected area of 1×1 cm^2 were mounted. This is a conventional procedure and has been described elsewhere.[6]

Reagent-grade chemicals and Milli-Q water (Millipore Corp.) were used in the electrolyte preparations. The electrolytes used were aqueous solutions of 0.1 N NaOH, 0.5 N $NaClO_4$ of different pH values buffered with K_2HPO_4/NaOH (pH 9.6) and K_2HPO_4/KH_2PO_4 (pH 6.8 and 4.7), and 0.1 N $HClO_4$. They were thoroughly purged with N_2 prior to and during measurements.

2. Electrochemistry. All electrochemical experiments were carried out at room temperature in the dark. A conventional three-electrode cell was employed in the experiments. The nanostructured TiO_2 electrode acted as the working electrode, a platinum grid in a separate compartment as the counter

10.1021/jp0036083 CCC: $20.00
Published on Web 03/13/2001

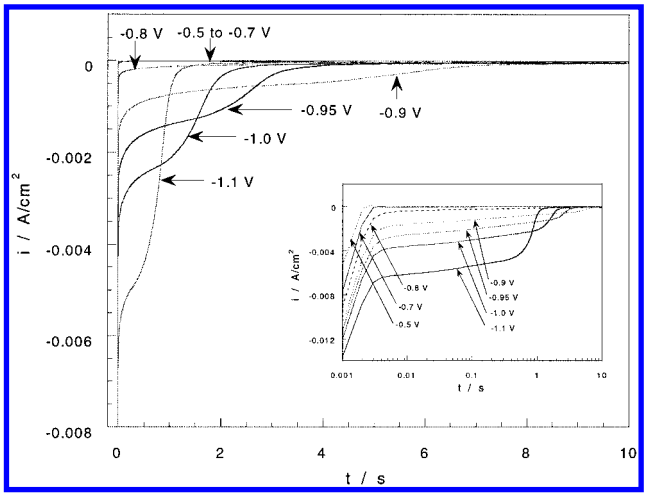

Figure 1. Transient current decays after resting a 5 μm thick nanostructured TiO_2 electrodes in 0.1 N NaOH at 0 V vs Ag/AgCl for 5 min and then shifting the potential to different potentials positive of the flat band. The electrolyte was purged with nitrogen gas and heavily stirred. The insert shows the results in semilogarithmic plot.

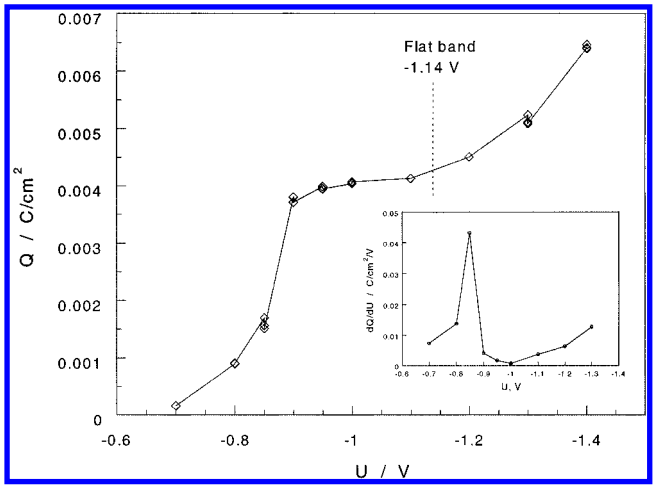

Figure 2. Cathodic charges accumulated at different potentials as derived by integrating the current−time curves in 0.1 N NaOH solution. The insert shows charge distribution against potential. The electrolyte was purged with nitrogen gas and heavily stirred.

electrode, and a saturated Ag/AgCl electrode (SSE) from Metrohm AG (Switzerland) in another separate chamber as the reference electrode. All potentials (U) are hereafter given with reference to the SSE electrode. According to the manufacturer's specification, this reference electrode has a potential of 197.0 mV vs normal hydrogen electrode (NHE) at 25 °C. An Autolab μII potentiostat (Eco Chemie BV) controlled by a personal computer was utilized to control the electrochemical measurements. The switch time of the potentiostat was 1 μs.

Chronoamperometry was used to investigate the transient current response (i) versus time (t). In 0.1 N NaOH, the nanostructured TiO_2 electrode was first polarized at 0 V for 5 min, and then the potential was shifted immediately to a preset value positive of U_{FB} and the transient current was registered. Similarly, in 0.5 N $NaClO_4$ (pH 4.7) solution, the electrode was polarized at 1 V for 5 min, and then the potential was shifted to a preset value positive of U_{FB} and the transient current was collected. Adapting the flat band potential for nanostructured TiO_2 given in the literature,[21] U_{FB} values of −1.14 V at pH 13 and −0.65 V at pH 4.7 were calculated and used as a base for selecting the preset potentials in experiments. Due to the restriction in data capacity of the software, a sampling time of 1 ms was selected in these experiments.

To investigate the effect of pH of the electrolyte on the behavior of nanostructured TiO_2, linear voltammetry (LV) was used. In these experiments, unbuffered solutions of 0.1 N NaOH and 0.1 N $HClO_4$ and buffered solutions of 0.5 N $NaClO_4$ (pH 9.6, 6.8, and 4.7) were used. Before the scanning, the electrodes were stabilized at appropriate positive potentials for 5 min. The potentials for such pretreatment were 0.5 V in 0.1 N NaOH, 1.25 V in 0.1 N $HClO_4$, 1 V at pH 4.7, 0.85 V at pH 6.8, and 0.75 V at pH 9.6, respectively. These selected potentials follow a Nernstian shift with the pH of the electrolyte. Then linear scans started at these potentials and were scanned to the negative potentials. A scanning rate of 2 mV/s was selected in all of these experiments.

Results and Discussion

1. Transient Currents in 0.1 N NaOH. In 0.1 N NaOH solution, the registered transient currents (i) of the nanostructured TiO_2 electrodes when shifted from 0 V to different potentials are shown in Figure 1. As soon as a negative potential is applied, a sharp cathodic current peak is observed. The current then decays very quickly. A semilogarithmic plot of i vs log t reveals that the initial current decay has a similar development with time. (See the initial linear part of the curves in the insert of Figure 1.) The slopes are within experimental error the same at all potentials. This decay is associated with the RC response on reorganization of interfacial charges in the system. Then, the transient is significantly influenced by the applied potential. At potential −0.5 to −0.7 V, the transient currents decrease to almost zero within a few milliseconds. At −0.8 V, there appears a slow process after the initial fast decay. The transient at −0.9 V shows a remarkable behavior. A two-step decay, with a distinct plateau region between, is observed. This behavior is found at all potentials negative of −0.9 V, with the only difference that the plateau region of the current is shorter at more negative potentials. The results above can be understood in terms of trap filling in the band gap region. Nanostructured TiO_2 has a flat band potential of −1.14 V at pH 13.[21] At potentials positive of −0.7 V, the density of traps is low, and thus the trap-filling time is short. This results in fast decay of the transient current.[30] Between −0.7 and −0.8 V, the trap density increases. More traps are present in this region and a longer time is required to fill these traps. When the potential is close to the flat band level, however, the density of traps decreases again. Figure 1 indicates that most of the traps are located positive of −0.9 V. This results in a long trap-filling time at −0.9 V. A further negative shift of the potential significantly shortens the trap-filling time. This should be related to the kinetics of trap filling. A faster trap filling is expected at a more negative potential (at a higher energy level) since the driving force for the trap filling is larger.

When the accumulated charge (Q) under the transient current−time curves in Figure 1 is calculated, (we include also the fast transient in the initial decay, as the integrated charge in this range is almost negligible), some interesting features appear. Figure 2 shows the accumulated charge, Q, at different potentials. At potentials positive of −0.7 V, the accumulated charge is very small. It clearly indicates that there is a sharp increase in accumulated charge up to −0.9 V. At potential negative of −0.9 V, the accumulated charges saturates, resulting in a plateau in the Q vs U curve (Figure 2).

Assuming that the accumulated charge, Q, by trap-filling reflects the density of states, we can write

$$Q = q\int_{E_F^\circ}^{E_F} N_{trap}(E)\,dE \quad (1)$$

where $N_{trap}(E)$ is the trap density as a function of energy (cm^{-3} eV^{-1}), E_F° is the Fermi level at the initial potential U_F° well below the trap levels, E_F is the Fermi level at the preset potential U, and q is the elementary charge. Since $E_F - E_F^\circ = -q(U - U_F^\circ)$, the trap density is expressed by

$$N_{trap}(E) = -\frac{1}{q^2}\frac{dQ}{dU} \quad (2)$$

The trap density can, of course, also be expressed as a function of the potential, i.e.

$$N_{trap}(E)\,dE = -N_{trap}(U)\,dU \quad (3)$$

where $N_{trap}(U)$ is the trap density as a function of potential (cm^{-3} V^{-1}). The transfer of trap density between the energy scale and the potential scale is

$$N_{trap}(E) = -\frac{N_{trap}(U)}{q} \quad (4)$$

Combining the above, one obtains

$$N_{trap}(U) = \frac{1}{q}\frac{dQ}{dU} \quad (5)$$

Equation 5 clearly indicates that trap density is directly proportional to dQ/dU, which provides a direct measure of trap distribution. By calculating the derivative of the accumulated charge vs the applied potential, a plot of dQ/dU vs U is obtained, shown in the insert of Figure 2. This plot reflects the distribution of traps. It is seen that most traps are located at potentials more positive than −0.9 V.

From the average accumulated charges ($Q \approx 0.0040$ C/cm^2) in the saturation region (−0.9 to −1.1 V), a value of totally trapped electrons per projected film area of a 5.0 μm thick film was estimated to be 2.5×10^{16} cm^{-2}. Adopting a roughness factor of 500,[6] we obtain a total trap density of 5×10^{13} cm^{-2} of inner surface area. This result is in agreement with some of the previous investigations,[21,27] but is about 20−50 times higher than some other investigations where 1×10^{12} cm^{-2} is a typical value.[8,14,16,17] As we will see below, the trap density is strongly pH dependent, and the density varies with orders of magnitude with the pH. The disagreement we observe between different investigations could thus be related to the pH of the electrolytes used by the different investigators.

When the potential is shifted further negatively to potentials above the flat band, the accumulated charges increase again (Figure 2). This can be understood in terms of conduction band filling. The point where the increase starts seems to coincide well with the flat band level of −1.14 V at pH 13.[21] See the dashed line in Figure 2. The insert in Figure 2 indicates that trap-filling process ends at −1.0 V while conduction band filling starts at potentials negative of −1.1 V.

2. Transient Currents in pH 4.7 $NaClO_4$. Transient currents in the pH 4.7 solution are shown in Figure 3. A behavior similar to that in the pH 13 solution is registered, with the only difference that now the transient currents are much lower. Again, a trap-filling process is observed at potentials negative of the level where most traps are located (around −0.3 V). Comparing to Figure 1, it is noticed that the trap-filling process is faster in the pH 4.7 solution than that in pH 13 solution.

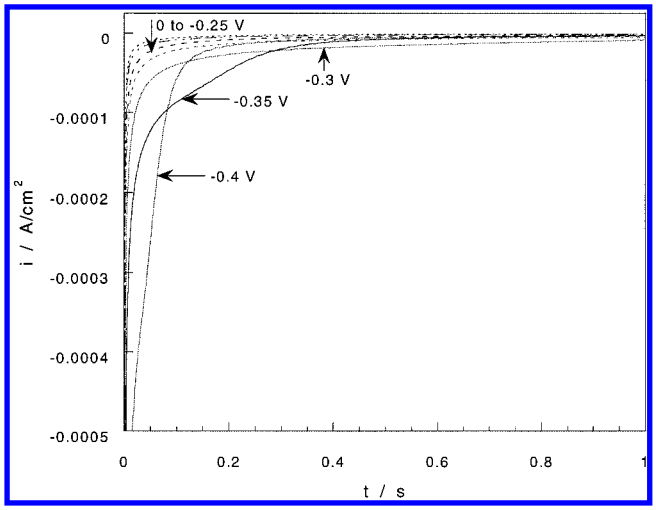

Figure 3. Transient current of the same kind as in Figure 1 of 5 μm thick nanostructured TiO_2 electrodes in 0.5 N $NaClO_4$ at pH 4.7. The electrode was initially rested at 1 V vs Ag/AgCl for 5 min and then shifted to different applied potentials positive of the flat band. The electrolyte was purged with nitrogen gas and heavily stirred.

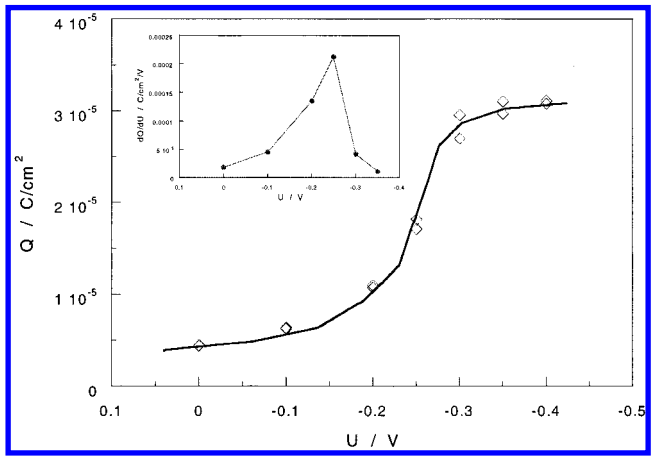

Figure 4. Cathodic charges accumulated at different potentials as derived by integrating the current−time curves in the solution at pH 4.7. The electrolyte was purged with N_2 and heavily stirred. The insert shows dQ/dU distribution against potential.

Figure 4 shows the charge required to fill the traps, which is only about 1/100 of that required for the trap filling in the pH 13 solution (Figure 1). The accumulated charge saturates at potentials negative of −0.3 V, indicating that in the pH 4.7 solution most traps are located at potentials positive of −0.3 V. The derivative of the accumulated charge vs the applied potential is also calculated and plotted in the insert of Figure 4. Similar to the insert of Figure 2, the insert plot of Figure 4 reflects the trap distribution at pH 4.7. By calculating the charge consumed in the potential range −0.3 to −0.4 V, the total amount of trapped electrons was estimated to be 1.9×10^{14} cm^{-2} of the 5.0 μm thick film. With the same assumption about the roughness factor as above, the total trapping density at pH 4.7 was estimated to 4×10^{11} cm^{-2}. This result is in agreement with previous investigations for similar nanostructured TiO_2 electrodes using intensity-modulated photovoltage,[8] photocurrent spectroscopy,[17] and electrochemical spectroscopy.[14]

3. Effect of pH of the Electrolytes. The above estimation of trapping density leads us to consider the origin of traps, which has been related to the grain boundaries or to the NSEI.[17] Comparing trap densities at different pH values, it is noticed that much lower values are obtained in neutral and acid electrolytes. To get detailed information on this point, the

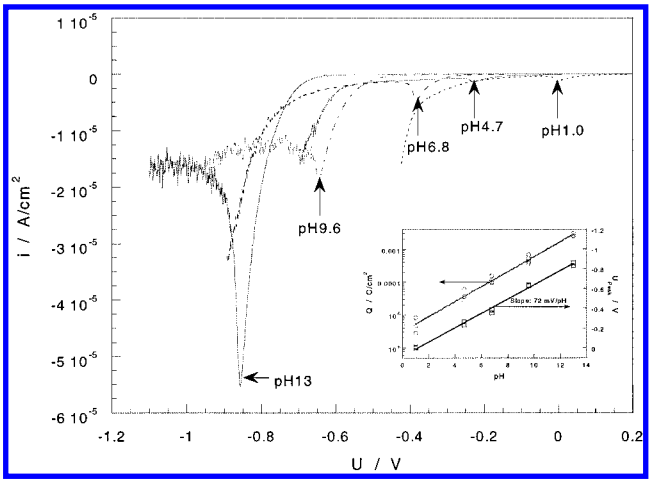

Figure 5. Effect of pH of the electrolyte on the electrochemical behavior of 5 μm thick nanostructured TiO_2 film electrodes. The electrolytes were purged with nitrogen gas and heavily stirred. The scan rate was 2 mV/s, and the scans started from the positive potential end. The insert shows the shift of cathodic peaks and the estimated charge accumulation in these peaks against pH of the electrolytes.

current−potential characteristics (or LV) of the TiO_2 film electrode were recorded at different pH values. The results are shown in Figure 5. It is interesting to note that each curve has a cathodic peak, similar to what was observed in earlier investigations.[14,29]

To explain the peaks in Figure 5, we re-treat eq 5 as

$$N_{\text{trap}}(U) = \frac{1}{q}\frac{\mathrm{d}Q/\mathrm{d}t}{\mathrm{d}U/\mathrm{d}t} = \frac{1}{q}\frac{i}{\mathrm{d}U/\mathrm{d}t} \qquad (6)$$

where i is the current density, t is time, and $\mathrm{d}U/\mathrm{d}t$ is the scanning rate in a linear sweep voltammmetry. Equation 6 illustrates that the trap distribution at constant scanning rates is directly proportional to the collected current density. Alternatively, current density distribution is a direct measure of trap density. Thus a simple LV provides an easy method to investigate the trap distribution in nanostructured electrodes. Since the scanning rate was the same for all the experiments, the curves in Figure 5 make it possible to compare the trap distribution at different pH values. We can also compare the curves at pH 13 and 4.7 with the inserts in Figures 2 and 4. We clearly see that they are in good agreement. The size of the peak increases dramatically with increasing pH, which strongly indicates that the traps investigated are surface-related traps. The peaks shift to negative potentials with increasing pH. This behavior is shown in the insert of Figure 5, where the cathodic peak potential, U_{peak}, is plotted vs pH. This plot yields a slope of 72 mV/pH, which indicates that the behavior basically obeys the Nernstian relationship. The insert of Figure 5 also gives the relationship of accumulated charge due to traps, which was integrated approximately from the LV curve under the cathodic peaks, vs pH of the solution. It seems that the relationship is exponential. In other words, the charge decreases with the proton concentration in the solution. By fitting the points in the insert of Figure 5, we have

$$Q \approx 3.0 \times 10^{-6}\, \mathrm{e}^{0.53\,\mathrm{pH}}\ [\mathrm{C\ cm^{-2}}] \qquad (7)$$

or

$$Q \approx 3.0 \times 10^{-6}[\mathrm{H^+}]^{-0.23} \qquad (8)$$

where $[H^+]$ represents the proton concentration in the solution, which was converted from the pH of the solution. Both have a relation coefficient better than 0.99. The reason for such behavior is far from understood. The value 0.23 is close to 1/4. Whether this is just coincidental or can be explained by considering simple equilibria in the system is not clear at present.

Further work is in progress to investigate the effect of other cations, since previous research on solar cells reveals the effect of cations.[31] We will also look deeper into the effect of dioxygen, since adsorption of dioxygen at TiO_2 is a common phenomenon.[32]

Finally it should be noted that the present experimental results are in conflict with the model recently presented by van de Lagemaat and Frank,[33] who, on the basis of data from intensity-modulated photovoltage spectroscopy (IMPS) and TOF measurements,[8,34] assume an exponential distribution of surface states. The following questions arise: What is the difference between the method used to determine the distribution and density of surface states in the present work, compared to IMPS and TOF measurements? Are the systems investigated fundamentally different? Does the model proposed by van de Lagemaat and Frank discriminate between an exponential distribution and the more "Gaussian shaped" distribution we observe, if the latter is so narrow and positioned so close to the CB (<0.3 V) as we observe? It would be interesting to see if Gaussian shaped distribution of the type we find could be fitted to data of the kind van de Lagemaat and Frank present in Figure 2 of ref 33.

Conclusions

Electrons trapped in nanostructured TiO_2 (anatase) can be observed by means of electrochemical methods. The transient current decays registered at different applied potentials clearly indicate a trap-filling process. Most traps locate positive of −0.9 V at pH 13 and positive of −0.3 V at pH 4.7. The trap densities per unit area of the inner surface of the nanostructured TiO_2 were estimated to be 4×10^{11} and 5×10^{13} $\mathrm{cm^{-2}}$ at pH 4.7 and 13, respectively. The pH dependency of the trap density indicates that traps investigated are surface-related. The relationship between trapped charge and the proton concentration is expressed by $Q \approx 3.0 \times 10^{-6}[\mathrm{H^+}]^{-0.23}$.

Acknowledgment. This work has been supported by the Swedish National Energy Administration and the Swedish Research Council for Engineering Sciences (TFR).

References and Notes

(1) O'Regan, B.; Grätzel, M. *Nature* **1991**, *353*, 737.
(2) Bedja, I.; Hotchandani, S.; Kamat, P. V. *J. Phys. Chem.* **1994**, *98*, 4133.
(3) Schwartzburg, K.; Willig, F. *Appl. Phys. Lett.* **1991**, *58*, 2520.
(4) Södergren, S.; Hagfeldt, A.; Olsson, J.; Lindquist, S.-E. *J. Phys. Chem.* **1994**, *98*, 5552.
(5) Fitzmaurice, D. *Sol. Energy Mater. Sol. Cells* **1994**, *32*, 289.
(6) Hagfeldt, A.; Grätzel, M. *Chem. Rev.* **1995**, *95*, 49.
(7) Boschloo, G. K.; Goossens, A. *J. Phys. Chem.* **1996**, *100*, 19489.
(8) Schlichthörl, G.; Huang, S. Y.; Sprague, J.; Frank, A. J. *J. Phys. Chem. B* **1997**, *101*, 8141.
(9) Huang, S. Y.; Schlichthörl, G.; Nozik, A. J.; Grätzel, M.; Frank, A. J. *J. Phys. Chem. B* **1997**, *101*, 2576.
(10) Schwarzburg, K.; Willig, F. *J. Phys. Chem. B* **1999**, *103*, 5743.
(11) Yan, S. G.; Hupp, J. T. *J. Phys. Chem.* **1996**, *100*, 6867.
(12) Fisher, A. C.; Peter, L. M.; Ponomarev, E. A.; Walker, A. B.; Wijayantha, K. G. U. *J. Phys. Chem. B* **2000**, *104*, 949.
(13) Könenkamp, R.; Henninger, R.; Hoyer, P. *J. Phys. Chem.* **1993**, *97*, 7328.
(14) Boschloo, G.; Fitzmaurice, D. *J. Phys. Chem. B* **1999**, *103*, 2228.
(15) Franco, G.; Gehring, J.; Peter, L. M.; Ponomarev, E. A.; Uhlendorf, I. *J. Phys. Chem. B* **1999**, *103*, 692.
(16) de Jongh, P. E.; Vanmaekelbergh, D. *Phys. Rev. Lett.* **1996**, *77*, 3427.

(17) de Jongh, P. E.; Vanmaekelbergh, D. *J. Phys. Chem. B* **1997**, *101*, 2716.
(18) Ward, M. D.; Bard, A. J. *J. Phys. Chem.* **1982**, *86*, 3599.
(19) Rotherberger, G.; Moser, J.; Grätzel, M.; Serpone, N.; Sharma, D. K. *J. Am. Chem. Soc.* **1985**, *107*, 8054.
(20) Howe, R. F.; Grätzel, M. *J. Phys. Chem.* **1985**, *89*, 4495.
(21) Rothenberger, G.; Fitzmaurice, D.; Grätzel, M. *J. Phys. Chem.* **1992**, *96*, 5983.
(22) Redmond, G.; Grätzel, M.; Fitzmaurice, D. *J. Phys. Chem.* **1993**, *97*, 6951.
(23) Haque, S. A.; Tachibana, Y.; Klug, D. R.; Durrant, J. R. *J. Phys. Chem. B* **1998**, *102*, 1745.
(24) Haque, S. A.; Tachibana, Y.; Willis, R. L.; Moser, J. E.; Grätzel, M.; Klug, D. R.; Durrant, J. R. *J. Phys. Chem. B* **2000**, *104*, 538.
(25) Hagfeldt, A.; Lindström, H.; Sodergren, S.; Lindquist, S.-E. *J. Electroanal. Chem.* **1995**, *381*, 39.
(26) Cao, F.; Oskam, G.; Searson, P. C.; Siripala, J. M.; Heimer, T. A.; Farzad, F.; Meyer, G. J. *J. Phys. Chem.* **1995**, *99*, 11974.
(27) Kay, A.; Humphry-Baker, R.; Grätzel, M. *J. Phys. Chem.* **1994**, *98*, 952.
(28) Boschloo, G. K.; Goossens, A.; Schoonman, J. *J. Electroanal. Chem.* **1997**, *428*, 25.
(29) Kavan, L.; Kratochvilová, K.; Grätzel, M. *J. Electroanal. Chem.* **1995**, *394*, 93.
(30) O'Regan, B.; Moser, J.; Anderson, M.; Grätzel, M. *J. Phys. Chem.* **1990**, *94*, 8720.
(31) Liu, Y.; Hagfeldt, A.; Xiao, X.-R.; Lindquist, S.-E. *Sol. Energy Mater. Sol. Cells* **1998**, *55*, 267.
(32) Linsebigler, A. L.; Lu, G.; Yates, J. T. *Chem. Rev.* **1995**, *95*, 735.
(33) van de Lagemaat, J.; Frank, A. J. *J. Phys. Chem. B* **2000**, *104*, 4292.
(34) Nelson, J. *Phys. Rev. B* **1999**, *59*, 15374.